

UDC 544.65

MAGNETRON DEPOSITION OF ANODE FUNCTIONAL LAYERS FOR SOLID OXIDE FUEL CELLS**A.A. Solovyev¹, I.V. Ionov¹, A.V. Shipilova¹, V.A. Semenov¹, E.A. Smolyanskiy²**¹*Institute of High Current Electronics SB RAS,
2/3 Akademichesky Ave., Tomsk, 634055, Russia, e-mail: andrewsol@mail.ru*²*Tomsk Polytechnic University,
30 Lenina Ave., Tomsk, 634050, Russia*

Abstract: *The proposed review is dedicated to the latest achievements in the field of magnetron deposition of thin-film anode functional layers (AFLs) for solid oxide fuel cells (SOFCs) of various designs (electrolyte-supported, anode-supported and micro-SOFC). Manufacturing of SOFCs components remains nowadays a key point for the industrial development of this electrochemical conversion device. Formation of thin nanostructured anodes by physical vapor deposition methods allows increasing efficiency of SOFCs due to the reduction of polarization losses at the anode. The review discusses the use of thin-film anodes for different SOFC configurations intended to work in low, intermediate and high temperature ranges. The influence of the deposition parameters, microstructure and chemical composition of AFLs on SOFC performance is analyzed.*

Keywords: *SOFC, anode functional layer, thin film, magnetron sputtering, polarization losses*

DOI:10.32737/2221-8688-2019-2-252-266

Introduction

Solid oxide fuel cells (SOFCs) are electrochemical devices that allow directly converting the chemical energy of fuel into electrical and thermal [1]. Due to the numerous advantages of SOFC, they are actively developing throughout the world. Within this topic, an urgent task is the development of medium-temperature, i.e. operating at 600–800 °C, anode-supported SOFC. The latter makes it possible to reduce internal losses in SOFC and increase the service life of power plants. Internal losses in SOFC consist mainly of ohmic losses in the electrolyte and activation losses in the electrodes. The former can be minimized by reducing the thickness of the electrolyte. Formation of nanostructured thin-film anodes with a developed three-phase boundary (TPB) "metal-ion conductor-fuel gas" allows reducing of activation losses in the anode [2,3]. SOFC anodes are metal ceramic composites consisting of a phase with oxygen ion conductivity (for example, yttria-

stabilized zirconia (YSZ) or gadolinium doped ceria (GDC)) and a phase with electronic conductivity (metal or alloy). In anode-supported SOFC, the anode consists of at least two layers: a current collector layer (about 500 microns thick) and a thin functional electrochemically active layer (about 15 microns thick). The current collector layer should have a porous structure sufficient to supply the fuel to the TPB and remove the reaction products. Also it should ensure high mechanical strength and electrical conductivity. An electrochemical reaction takes place in the functional layer. Its intensity depends on the operating temperature and the density of the three-phase boundary. As the operating temperature decreases, the activation losses in the anode and their contribution to the total resistance of the SOFC increase.

For the manufacture of SOFC anodes, methods such as slip-casting and screen printing are widely used. However, they

require long stages of high-temperature sintering, which can cause undesirable reactions between the SOFC layers, deformations, cracks. These methods make it difficult to manufacture anode functional layers (AFLs) with a particle size of less than 1 micron even when using nanopowders, due to the coarsening of particles during high-temperature sintering [4]. A high surface energy of nanopowders contributes to their excessive agglomeration. The methods of physical vapor deposition (PVD) do not have these disadvantages [5]. They make it possible to reduce the temperature of the formation of functional layers and to implement structures that, in principle, cannot be created using powder sintering methods. PVD includes methods based on target evaporation, ion-beam sputtering and ion-plasma sputtering. For the manufacture of SOFC layers, the most frequently used methods are electron-beam [6, 7] and laser evaporation, magnetron sputtering. The laser evaporation method is used to form electrolytes [8, 9] and anode functional layers of the anode-supported SOFC [10]. However, electron beam and laser evaporation do not allow the deposition of coatings on large area substrates. Among PVD methods, magnetron sputtering is the most promising method for SOFC fabrication. The advantages of this method are the possibility of independent regulation of the main parameters of the sputtering process, formation of uniform coatings with required characteristics, and the possibility of processing of large-area surfaces [11]. Regulating the process parameters such as particle energy, degree of ionization, substrate temperature, substrate bias voltage, deposition rate, gas pressure, discharge power and operating mode of the magnetron sputtering system makes it possible to produce dense or nanoporous coatings.

Deposition of anode functional layers for electrolyte-supported SOFC

When NiO/YSZ or NiO/GDC AFLs are formed by the reactive magnetron sputtering in the atmosphere of Ar + O₂, their microstructure, including porosity, can be regulated by the substrate temperature, deposition rate, particle angle of incidence,

working pressure [12]. The substrate temperature has the greatest influence on the structure of the material (amorphous or crystalline) and its phase composition. While the deposition rate, particle angle of incidence, working pressure, mainly affect the density of the coating (the presence of porosity). An important parameter is the ratio of Ar/O₂ in a vacuum chamber during reactive magnetron sputtering. The Ar/O₂ ratio of argon and oxygen affects the oxidation of the target during the sputtering process and, consequently, the target sputtering rate and film deposition rate. On the one hand, at low oxygen partial pressure, the film deposition rate is higher. However, the resulting film may have a lack of oxygen and then it will require high-temperature annealing in air. On the other hand, at high oxygen partial pressure, sputtering is carried out in the so-called "poisoned" mode. In this mode, the deposition rate of the film is minimal, but it has a stoichiometric composition.

NiO/YSZ AFL, for example, can be formed from two metal Ni and Zr/Y (86/14 at.%) targets by their joint sputtering, and one Ni/Zr/Y (68.8/26.6 /4.6 wt.%) target. The first method allows adjusting the content of Ni in the formed layer. But the second method is easier to implement.

In [13] Ni-YSZ films are deposited at room temperature by reactive magnetron sputtering from a single Ni/Zr/Y metallic target at rates as high as 4 μm h⁻¹. The bipolar pulsed voltage with the pulse frequency 100 kHz was used. The as-deposited film surface (Fig. 1,a,b) has granular morphology with small grains of 10 nm, and a cauliflower-like structure. The cross section shows that structure similar to cauliflower arises from a columnar structure, which is typical for magnetron sputtered films [14].

After annealing at 900 °C for 90 min NiO/YSZ film has a denser structure due to atomic reorganisation during heat treatment (Fig. 1,c,d). The cross-section is no longer columnar and grain boundaries are less distinguished. According to X-Ray diffraction analysis, before annealing, the film exhibited a poor crystalline quality. But after annealing at 900 °C, diffraction peaks

corresponding to the 8YSZ, NiO(200) and Ni(111) phases were detected. The microstructure of reduced thin-film anodes and their electrocatalytic properties were not studied.

Garcia-Garcia *et al.* [15] prepared

highly porous, columnar NiO/YSZ thin films by reactive pulsed DC magnetron sputtering (200 W, 80 kHz) with deposition at glancing incidence. The pressure during deposition was maintained at 5×10^{-3} mbar in a process gas that consisted of 40 sccm Ar and 2.5 sccm O_2 .

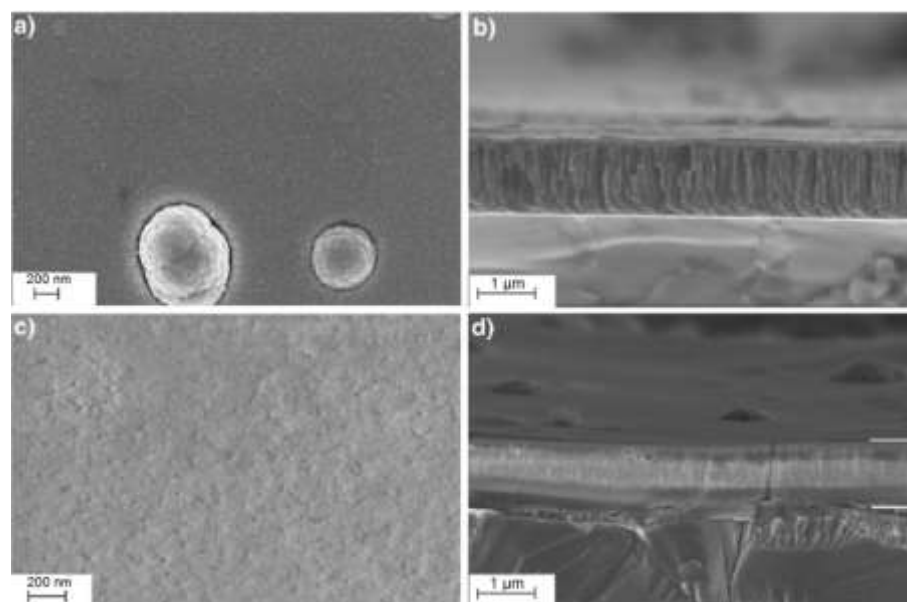


Fig. 1. SEM images of NiO/YSZ film as deposited (a, b) and after annealing at 900 °C for 90 min in air (c, d) [13].

The deposited at room temperature films were also essentially amorphous. Annealing such films at 850°C in hydrogen resulted in film crystallization with preservation of the columnar

structure. However, during the NiO reduction to metallic Ni latter was partially segregated to the film surface and formation of Ni agglomerates with a size of 0.7–2 μm (Fig. 2) was occurred.

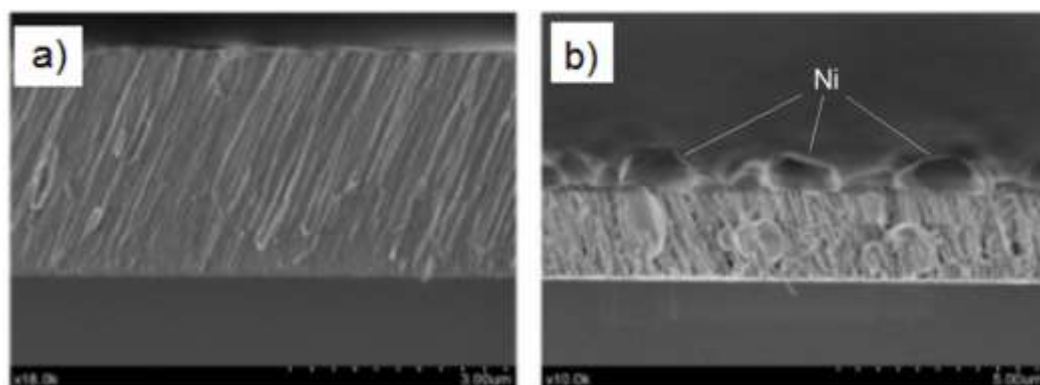


Fig. 2. Cross section of the as-deposited thin film (a) and after reduction in hydrogen (b). Silicon substrate [15].

Thus, the main disadvantage of nickel-based anode functional layers formed by PVD methods is the formation of nickel agglomerates on a

desurface during reduction in hydrogen [15]. The amount of agglomerates depends on the nickel content in the film. This phenomenon was also

observed for anodes formed by laser evaporation [10]. Ni agglomeration leads to a decrease in the three-phase boundary area at the anode [16] and can lead to the formation of cracks in the electrolyte film.

Agglomeration of particles of the Ni phase is usually related to the Ostwald ripening process [17]. This process may be based on the transport of Ni particles through the gas phase (evaporation and deposition) [18]. It is known that $\text{Ni}(\text{OH})_2$ has a six-fold evaporation rate as compared to that of Ni. Transport of Ni atoms could occur from small

granules to large ones by evaporation of $\text{Ni}(\text{OH})_2$.

To solve the problem of nickel agglomeration, the influence of annealing in an air atmosphere at temperatures of 800–1200 °C on the microstructure of NiO/YSZ films formed by laser evaporation was studied in [10]. Annealing at 1200 °C has been shown to prevent nickel agglomeration, due to the formation of a strong YSZ matrix, which inhibits the enlargement of nickel granules (Fig. 3).

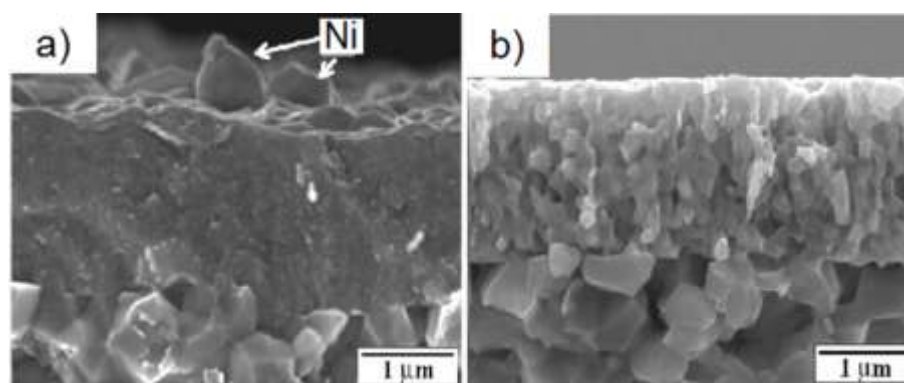


Fig. 3. Cross section of the PLD deposited NiO/YSZ films after reduction at 600 °C in 4% H_2 . a) without post-annealing, b) annealed in air at 1200 °C for 1 h [10].

In another work of Garcia-Garcia *et al.* [19] a ~5 μm Ni/YSZ anode was prepared on YSZ electrolyte by reactive pulsed magnetron sputtering at an oblique angle of incidence. Target-substrate distance was 5 cm with an angle of 80° between target

and substrate normal. A 50 mm diameter Ni/Zr/Y alloy (68.8/26.6/4.6 wt.%) target was used to produce Ni(50 vol.)/YSZ films at a discharge power of 200 W, 80 kHz frequency, working pressure of $5 \cdot 10^{-3}$ mbar and room temperature.

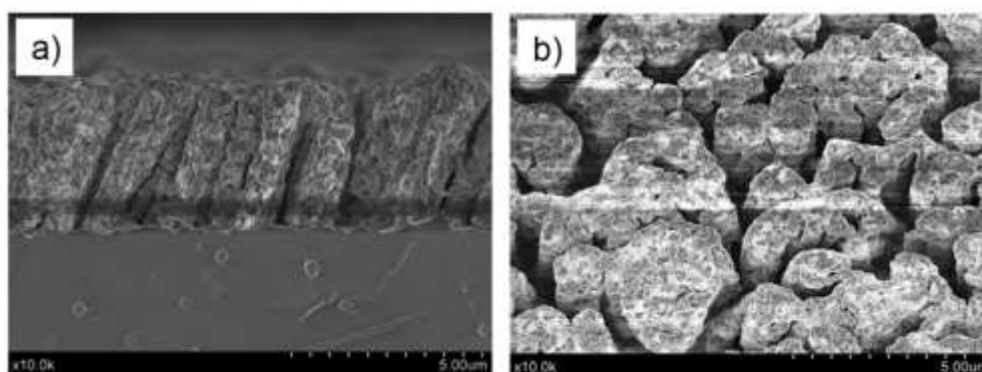


Fig. 4. SEM images of the cross section (a) and the surface (b) of the Ni/YSZ anode, deposited by magnetron sputtering at an angle to the substrate, after preliminary annealing at a temperature of 1250 °C in air and reduction in hydrogen at a temperature of 850 °C [19].

Deposition rate of $1.5 \mu\text{m h}^{-1}$ was achieved. It was shown that pre-annealing of the amorphous as-deposited NiO/YSZ film at 1250°C with the subsequent reduction produces a film consisting of uniformly distributed tilted columnar grains having extensive three-phase boundaries (Fig. 4). The performance of thin film anode was comparable to that of the commercial anode $50 \mu\text{m}$ thick (FuelCellMaterials (USA)), which was 10 times thicker and prepared by the doctor blade procedure. Single cell based on commercially available solid oxide half-cell comprising YSZ electrolyte and cathode (20 mm Single Electrode Cell - Cathode Only, FuelCellMaterials, USA) with magnetron sputtered NiO/YSZ anode had maximum power density of about 450 mW cm^{-2} at 850°C .

In order to increase the efficiency of thin-film anodes Garcia-Garcia *et al.* [20] suggested producing Ni-containing anodes comprising alternating layers of GDC and YSZ of 200 nm thickness. Also hybrid anode produced by co-deposition of Ni/YSZ and GDC were tested. The conditions for the deposition of layers did not change as compared with the previous works of the authors [15, 19]. In the as-deposited state, multi-layer anodes exhibited the highly porous columnar architecture, with well-defined boundaries between the NiO/YSZ and NiO/GDC layers (Fig. 5,a). The columnar structure was preserved after annealing in air (Fig. 5,b). As shown in Fig. 5,c, after the final reduction, highly porous thin anodes with pronounced columnar architecture were obtained.

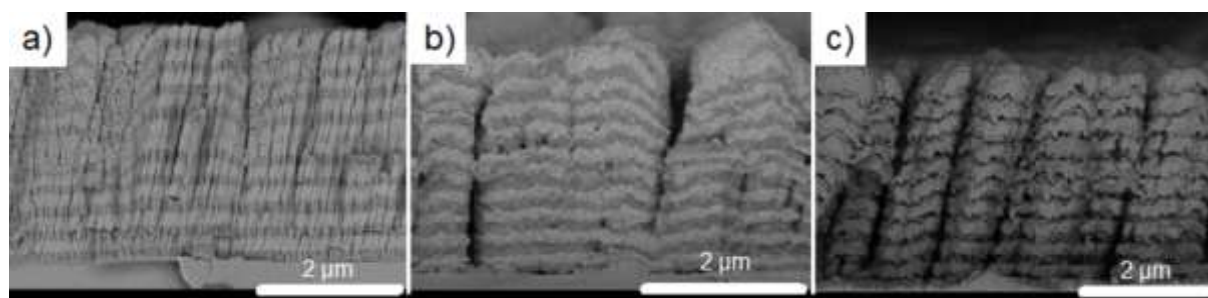


Fig. 5. SEM cross-section images of multi-layer thin-film anodes: a) as-deposited, b) annealed in air, c) reduced in hydrogen [20].

After subsequent fuel cell testing, the porous columnar architecture of the two-component layered thin film anodes was maintained and their resistance to delamination from the underlying YSZ electrolyte was superior to that of corresponding single component Ni-YSZ and Ni-GDC thin films. The performances of the multi-layer and hybrid anodes were almost the same and far superior to the single component YSZ and GDC anodes and also superior to the conventional commercially available thick anodes. Maximum power density of about 600 mW cm^{-2} at 850°C is achieved with hydrogen as fuel.

In another work Garcia-Garcia *et al.* [21] showed that thin Ni-GDC anodes exhibit excellent transport properties, robust under thermal cycling, and have good adhesion to the

YSZ electrolyte. Similarly prepared Au-doped Ni-GDC anodes exhibited the same morphology, porosity, durability and electrochemical performance (power density of about 500 mW cm^{-2} at 850°C in hydrogen). However, under steam reforming conditions with $\text{CH}_4/\text{H}_2\text{O}$ mixtures the behaviour of the Au-doped Ni-GDC anodes were far superior, exhibiting retention of good power density and dramatically improved resistance to deactivation by carbon deposition (Fig. 6).

Tanveer *et al.* [22] suggested using thin nickel-samarium-doped-ceria (Ni-SDC) anodes prepared by magnetron sputtering for intermediate temperature electrolyte-supported solid oxide fuel cells. The anode was deposited by radio-frequency sputtering on a $150 \mu\text{m}$ scandia-stabilized-zirconia (SSZ) substrate at room temperature.

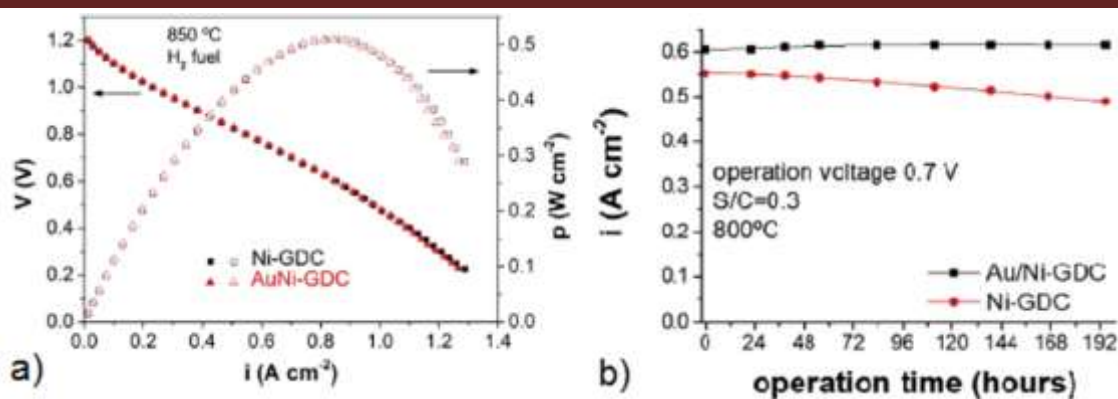


Fig. 6. The V–I and P–I characteristics of single cells with Ni-GDC and Au/Ni-GDC anodes obtained at 850 °C with hydrogen as fuel (a). I-t behavior of single cells with Ni-GDC and Au/Ni-GDC anodes operated at 0.7 V polarization voltage, 800 °C and steam to carbon ratio S/C = 0.3 [21].

The deposition process lasted for 5 hrs at a constant power of 100 W, and pressure of 50 mTorr. To analyze the effect of reactive O₂ gas on the anode manufacturing process, two different background gases were used during deposition, mixture of Ar/O₂:8/2 and Ar. Both methods resulted in producing nano-porous Ni-SDC films after reduction in H₂. But the reactively sputtered anodes have a 20% slower growth rate than the non-reactively sputtered ones. Also, the presence of this amount of oxygen in the sputtering chamber resulted in producing lesser catalytic Ni in the anodes. This resulted in a poorer performance for the cells containing reactively sputtered anodes when compared to nonreactive ones. Anodes were not annealed in air after deposition; therefore, agglomeration of Ni was observed on the anode surface after cell testing. LSM/YSZ cathode was screenprinted on the other side of the electrolyte. Peak power densities for such cells were 240, 140 and 50 mW cm⁻² at 800, 700 and 600 °C.

Jou and Wu [23] investigated thin Ni/YSZ anodes fabricated by reactive co-sputtering of a Ni and a Zr–Y target, followed by sequentially annealing in air at 900 °C, as part of an YSZ electrolyte-supported SOFC. A distinctive feature of the study was conducting test in a single-chamber configuration, in a mixture of CH₄ and air (CH₄:O₂ volume ratio = 2:1) at 700 °C. The maximum power density of the SOFC using the triple-layered Ni–YSZ thin film as the anode was 1.14 mW cm⁻², which was larger than that of 0.76 mW cm⁻², obtained using a screen-printed 20-mm-thick Ni/YSZ anode.

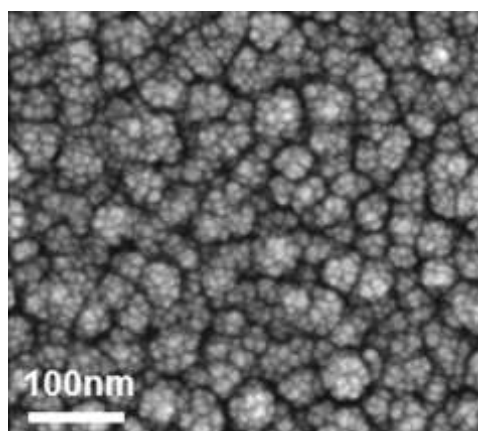


Fig. 7. Surface SEM image of Ru/CGO film deposited on YSZ/Si₃N₄/Si substrate (nominal volumetric ratio of Ru/CGO = 7/3) [24].

Deposition of anode functional layers for micro-SOFC

Takagi *et al.* [24] demonstrated that magnetron sputtered anodes could be used in micro-solid oxide fuel cells (μ SOFCs) also. Ruthenium and gadolinia-doped ceria (Ru/CGO) composite nano-crystalline thin film anodes were synthesized by co-sputtering from Ru metal (DC power) and CGO oxide (RF power) targets without substrate heating. Ru/CGO composite films on YSZ/Si₃N₄/Si substrate showed highly granular morphology with primary grain sizes of ~ 10 nm and secondary particles or pillars as large as 70–100 nm as shown in Fig. 7.

Stress-relaxed composite thin film anodes were developed on self-supported μ SOFCs with YSZ thin film electrolytes and porous platinum cathodes. μ SOFCs were

tested with room temperature humidified methane as fuel and air as the oxidant. They exhibited an open circuit voltage of 0.97 V and a peak power density of 275 mWcm⁻² at 485 °C.

Deposition of anode functional layers for anode-supported SOFC

In the works described above, thin-film anodes were mainly deposited on the electrolyte discs for the use in electrolyte-supported SOFCs. However, as was shown by us, thin-film anodes can also be used in anode-supported SOFC to reduce the polarization resistance at the anode [25]. The idea is to increase the characteristics of the anode-supported cells (ASC) by forming a thin-film anode functional layer between the thin-film electrolyte and commercial tape casted anode, as shown in Fig. 8.

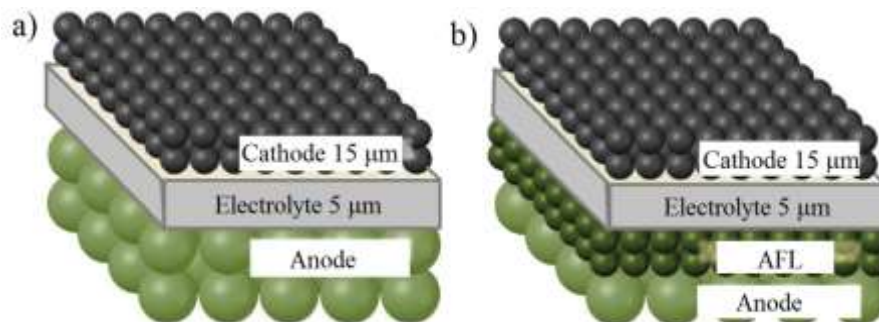


Fig. 8. The schematic of anode-supported cell configuration: a) conventional, b) with thin anode functional layer.

To study the influence of thin AFL on SOFCs' performance, single cells with and without AFL were fabricated. A 2 cm in diameter and 0.4-mm-thick NiO/YSZ anode supports cut out by laser from commercial anode sheets (Ningbo SOFCMAN Energy Technology, China) were used as substrates for magnetron deposition of both NiO/GDC and NiO/YSZ anode functional layers. AFLs were deposited by reactive co-sputtering of Ni, Zr_{0.86}Y_{0.14} and Ce_{0.9}Gd_{0.1} targets with diameter of 75 mm. The distance between the magnetron target center and substrate was 80 mm. Prior to film deposition, the substrates were heated to 400 °C. The deposited AFL samples were annealed in air atmosphere at different temperatures (600–1200 °C) for 1 h. For a good thermo-

mechanical compatibility with the electrolyte, the cells with NiO/GDC AFL were tested with GDC electrolyte, while cells with NiO/YSZ AFLs were tested with YSZ electrolyte. Electrolyte layers 4- μ m-thick were also deposited by reactive magnetron sputtering. The details of this process were described in our previous work [26]. The LSCF/GDC cathode layer was prepared on all cells by a screen-printing method using La_{0.6}Sr_{0.4}Co_{0.2}Fe_{0.8}O₃/Ce_{0.9}Gd_{0.1}O₂ paste (CERA-FC, Korea). The cathode area was 1 cm². Cathode sintering was performed at a temperature of 800 °C for 1 h before the fuel cell electrochemical test.

Analysis of cross-sections of Ni/YSZ and Ni/GDC AFLs (Fig. 9) showed that the composite films acquire a finely

porous structure after reduction in hydrogen. For all samples, a good contact of the AFL layer was observed.

both with an anode substrate and with an electrolyte layer.

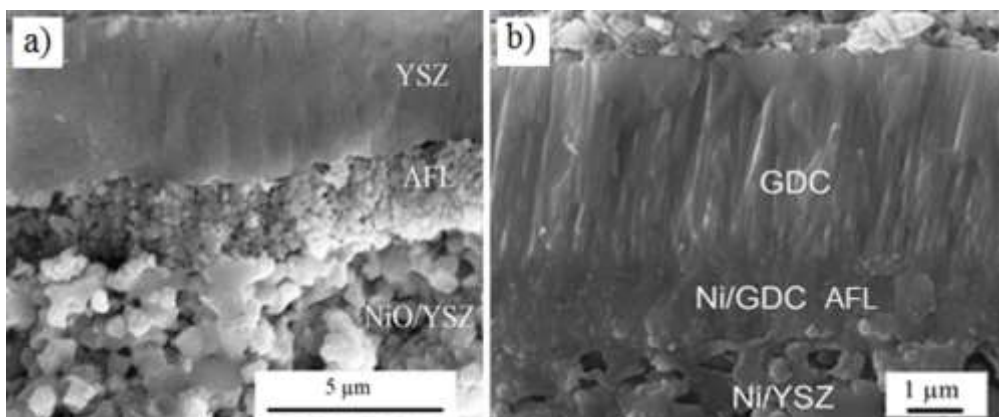


Fig. 9. Cross sectional SEM images of the SOFCs with nanostructured anode functional layers: a) Ni/YSZ AFL (NiO 60 vol.%.), b) Ni/GDC AFL (Ni 40 at. %). SEM images were obtained after cells testing [25].

The grain size and pore size of AFLs are hundreds of nanometers, in contrast to the substrate having micron-sized grains and pores. AFLs have a relatively smooth and uniform surface that facilitates deposition of a high quality dense and thin electrolyte layer leading to reduction in resistive losses.

The electrochemical activity of a cermet anode with the given microstructure and materials depends on the volume and on the grain size [27]. Smaller grains increase the triple phase boundary length and, as a result, the polarization resistance decreases.

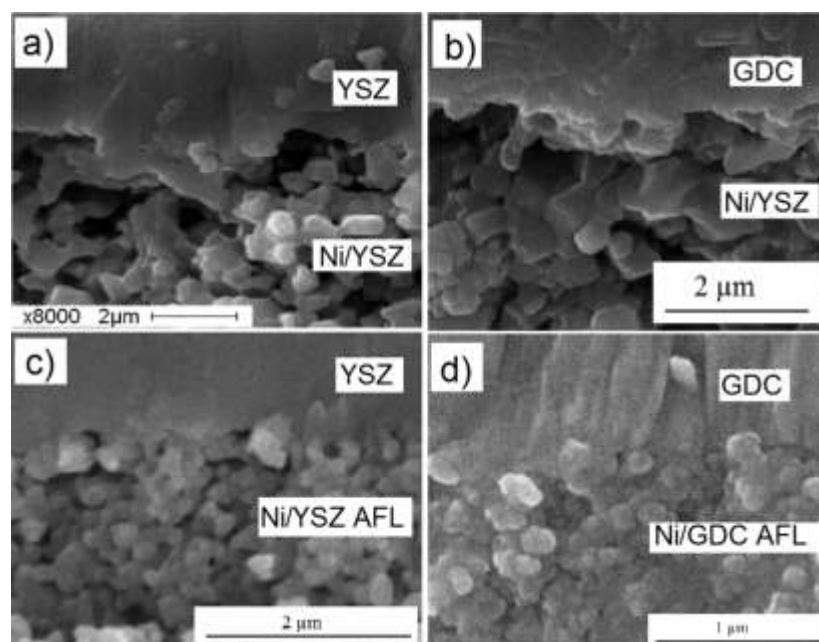


Fig. 10. Cross-sectional SEM images focused on the interface anode-electrolyte of the YSZ-based SOFCs without AFL (a), with AFL (c), and GDC-based SOFCs without AFL (b), with AFL (d) [25].

Figure 10 shows cross-sectional SEM images focused on the anode-electrolyte interface of the YSZ- and GDC-based SOFCs without and with anode functional layers. The fine and homogeneous microstructure of the AFLs enhances the continuity of the interface that should reduce interfacial polarization resistance. In order to estimate the impact of the NiO/YSZ and Ni/GDC AFL anode functional layers on the fuel cell performance, the current-voltage (I-V) and current-power (I-P) curves of the anode-supported cells with and without AFL were compared at different temperatures, as shown in Figs. 11 and 12.

The open circuit voltages (OCV) of cells with YSZ electrolyte were 1.08–1.17 V, depending on the temperature, that is close to the theoretical value of the SOFC. The peak power densities of the cell without AFL were 132, 469, and 950 mWcm^{-2} at 600, 700, and 800 °C, respectively. Single cell with magnetron sputtered NiO/YSZ AFL (NiO 60 vol. %) has peak power densities of 222, 675, and 1240 mWcm^{-2} at the same temperatures. Thus, the peak power density of fuel cells with the AFL is 30% higher at 800 °C and 68% higher at 600 °C than that of the cell without AFL. That is, the effect of AFL on the fuel cell performance is more pronounced at low temperatures.

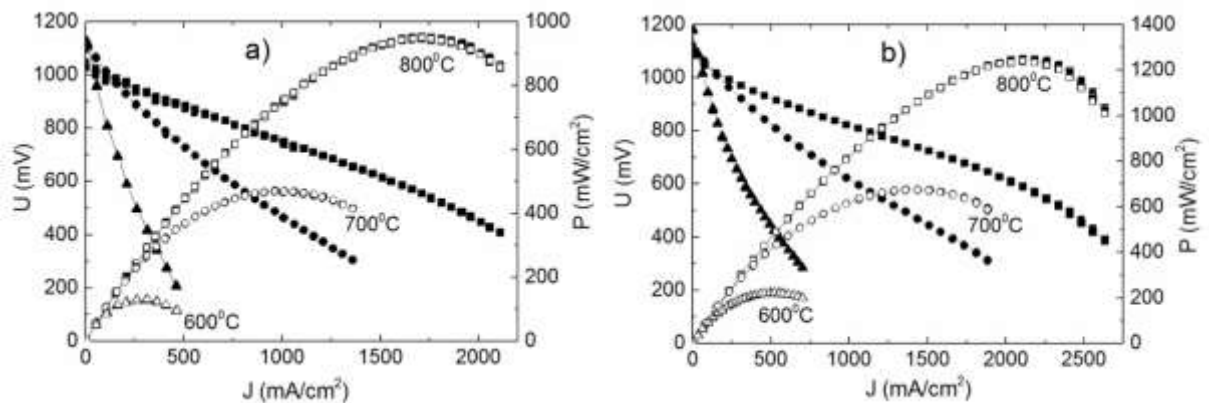


Fig. 11. I-V and I-P characteristics of the anode-supported SOFC with YSZ electrolyte and LSCF/GDC cathode without (a) and with (b) magnetron sputtered NiO/YSZ AFL (NiO 60 vol. %) measured at temperatures of 600–800 °C [25].

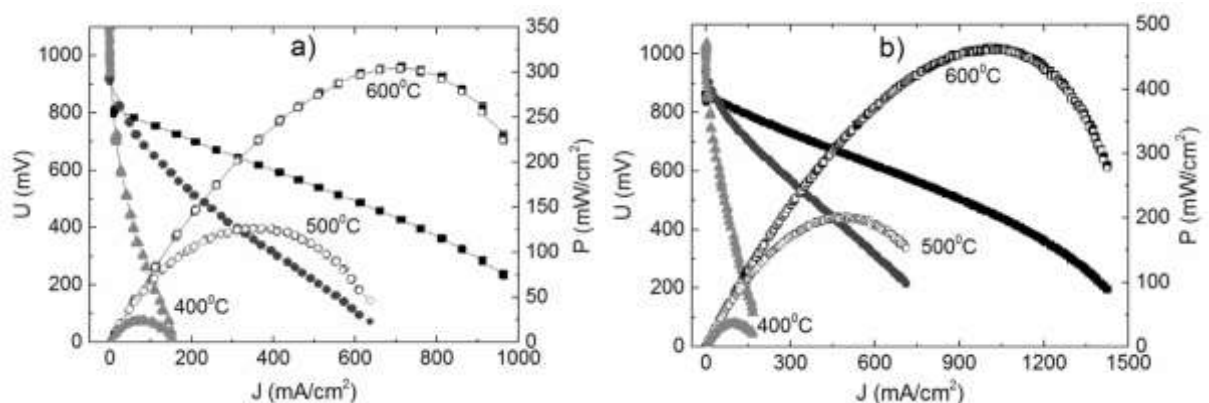


Fig. 12. I-V and I-P characteristics of the anode-supported SOFC with GDC electrolyte and LSCF/GDC cathode without (a) and with (b) magnetron sputtered NiO/GDC AFL (Ni 40 at. %) measured at temperatures of 400–600 °C [25].

The OCV values of the cells with GDC electrolyte were 1.134, 0.920, and 0.811 V at

400, 500, and 600 °C, respectively. The reduction of ceria from Ce^{4+} to Ce^{3+} in a

reducing atmosphere increases electronic conductivity, which decreases the open-circuit voltage of the cell. But at a temperature below 500 °C the electronic conductivity of GDC becomes negligible and OCV reaches high values comparable with YSZ electrolyte. The maximum power densities of cell without AFL were 25, 125, and 305 mWcm⁻² at 400, 500, and 600 °C, respectively. The OCV and maximum power densities of the cell with AFL were 1.037, 0.940, 0.861 V and 40, 200, 460 mWcm⁻² at 400, 500, and 600 °C, respectively. The increase in power density due to the formation of AFL is about 60% depending on the temperature.

The total area-specific resistance (ASR) of YSZ-based cell without AFL calculated from linear fit of I–V curve measured at 800 °C was 0.27 Ωcm². When AFL is applied, the ASR decreased to 0.2 Ωcm². The same dependence is observed when using NiO/GDC AFL. At 600 °C AFL deposition results in reduction of ASR from 0.54 to 0.38 Ωcm². This implies that a deposited NiO/YSZ and NiO/GDC AFLs reduced the total cell ASR by 26–30%.

Deposition of Cu-based SOFC anode functional layers

Ni-based anodes are usually used in solid oxide fuel cells when fuel is hydrogen. In this case anodes experience relatively low degradation rates and fast electrochemical kinetics. But if synthesis gas is used as fuel, Ni could be easily poisoned by contaminants like sulfur or carbon [28, 29]. Carbon deposition reduces the cell performance by blocking the anode reaction sites and damaging the microstructure of Ni in the anode. In recent

studies [30, 31], Cu has been suggested as an alternative to Ni as the electronic conductor in SOFC anodes. Recently, Cu/yttria stabilized zirconia (YSZ), Cu/samaria-doped ceria (SDC) and Cu/gadolinia-doped ceria (GDC) anodes [32–36] have been developed and tested, showing good electronic conductivity and tolerance towards sulfur-containing fuels. However, Cu has a low catalytic activity for hydrogen or hydrocarbon electrochemical oxidation, and so doped ceria should be used instead of YSZ in order to improve the cell performance.

Despite the advantages of Cu-based composite anodes, it is difficult to apply conventional ceramic processing methods to fabricate Cu-containing SOFCs due to the low melting point of Cu (that is 1085 °C). Presently they are manufactured using a multi-step wet ceramic technique that requires more processing and firing steps and not attractive for mass production. Furthermore, high sintering temperatures increase interdiffusion of elements between adjacent cell layers. To avoid the sintering of copper oxide at high temperatures, we proposed using magnetron sputtering for thin CuO/GDC anodes deposition.

CuO/GDC thin films were deposited by reactive magnetron co-sputtering of Cu and Ce_{0.9}Gd_{0.1} targets with diameter of 75 mm. Sputtering was carried out in oxygen-argon atmosphere at working pressure of 0.2 Pa in pulse bipolar mode at pulse repetition frequency of 80 kHz and positive pulse duration of 4 μs. The argon and oxygen flow rates were fixed at 26 and 33 sccm, respectively.

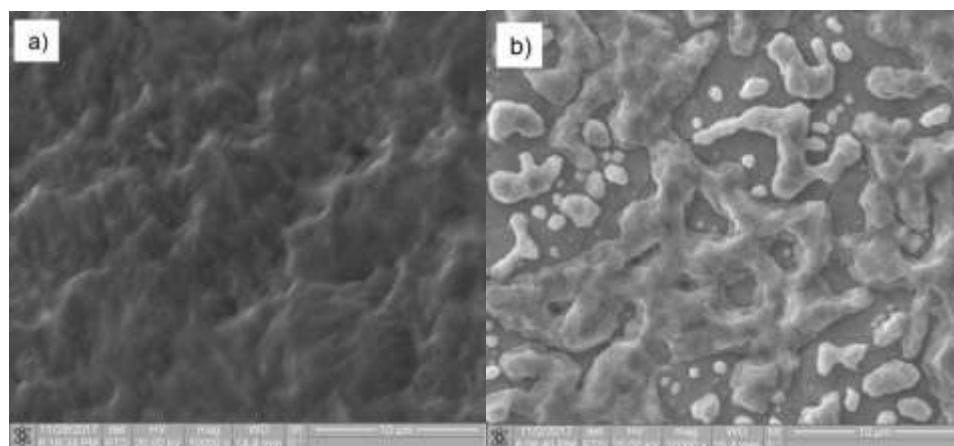


Fig. 13. Surface morphology of Cu/GDC film deposited on porous NiO/YSZ substrate (after reduction in hydrogen).

Targets were positioned at 45° to the fixed substrate holder. The distance between the magnetron target center and substrate was 80 mm. Prior to film deposition, the substrates were heated to 450 °C. The porous commercial NiO/YSZ anodes (SOFCMAN, China) with a thickness of 0.4 mm were used as substrates. The discharge power of a Ce-Gd magnetron was 1 kW. The discharge power of the Cu magnetron ranged from 100 to 700 W to control the volume content of CuO in the film. The copper content in the films was determined after films reduction in hydrogen. For example, at 500 W power of the Cu magnetron, the film contained 42 at. % of Cu.

Surface morphology of 2 μm thick Cu/GDC film (42 at.% of Cu) after reduction in H₂ at a temperature of 750 °C for 2 hours is shown in Fig. 13. As can be seen from the SEM image, Cu agglomeration occurs on the surface of the film, in analogy with what happens when nickel-containing thin films are

reduced at high temperature. In order to solve this problem, preliminary annealing of the films in air at 800 and 1000 °C was carried out, by analogy with Ni-based anodes.

Figures 14 and 15 show surface and cross-sectional images of thin-film CuO/GDC anodes deposited at power of Cu magnetron 500 W and annealed at a temperature of 800 and 1000 °C, respectively. After annealing, the samples were reduced in hydrogen. Both films formed intimate contact across the interface between the film and the substrate. Moreover, film/substrate interfaces are homogeneous. At an annealing temperature of 800 °C, agglomeration of copper into isolated particles having characteristic dimensions of less than 1 μm occurs on the surface of the film (Fig. 14,a). After annealing at 1000 °C, the absence of Cu agglomerates on the surface of the film and formation of a more porous structure of the film with local cracks of micron width on the surface is observed (Fig. 15,a).

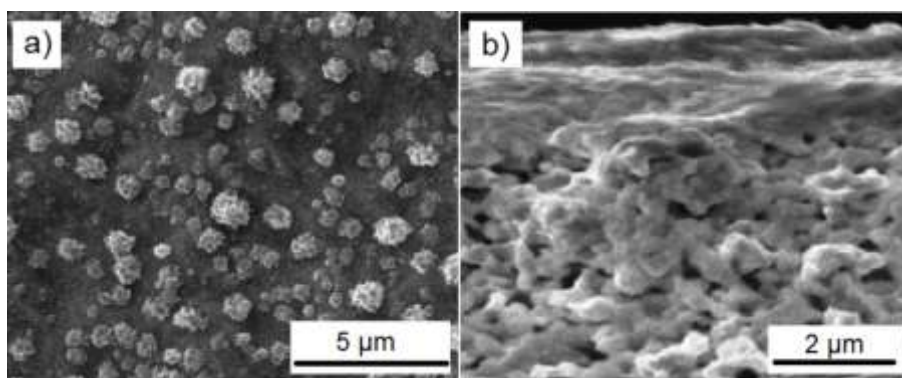


Fig. 14. Surface (a) and cross-sectional (b) SEM images of thin-film CuO/GDC AFLs annealed at a temperature of 800 °C in air and reduced in hydrogen (power of Cu magnetron - 500 W).

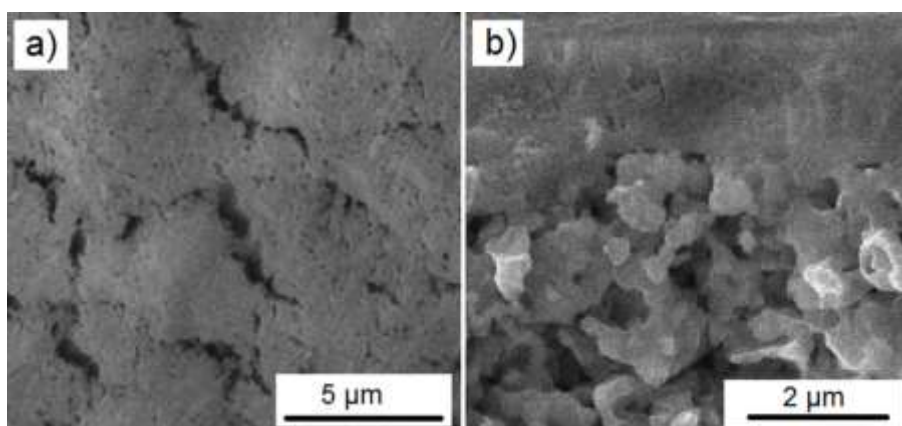


Fig. 15. Surface (a) and cross-sectional (b) SEM images of thin-film CuO/GDC AFLs annealed at a temperature of 1000 °C in air and reduced in hydrogen (power of Cu magnetron - 500 W).

These results show that magnetron sputtering is also a good technique for preparation of the thin-film copper-cermet anode material for SOFC. However,

electrochemical properties of magnetron sputtered CuO/GDC thin films are under investigation.

CONCLUSIONS

Uniform and porous composite thin films consisting of oxygen ionic conductive phase (YSZ or GDC) and electronic conductive phase (Ni or Cu) may be prepared by reactive magnetron sputtering. Annealing the as-deposited films in hydrogen resulted in NiO or CuO reduction to metallic Ni or Cu, which then segregated to the film surface with particles formation. However in the case of nickel based films, pre-calcination of the as-deposited films in air at 1200 °C followed by reduction produces films consisting of uniformly distributed nano-grains having extensive three-phase boundaries. The exceptionally high degree of dispersion and intermixing of the anode components promotes generation of very extensive three phase boundaries. Moreover, under thermal cycling in both oxidizing and reducing atmospheres, nickel based anode functional layers are robust against morphological changes and delamination from an YSZ substrate. Accordingly, because their thinness renders

them robust against strain-induced separation from the substrate, they are also promising candidates for use as highly conducting, stabilizing buffer layers for accommodating strain between conventional anodes and the YSZ electrolyte, and for fabrication of graded-composition Ni-YSZ anodes for use in SOFC applications. The SOFC performance is significantly increased using a nanostructured Ni/YSZ or Ni/GDC AFL as compared to the performance of cells without it. The increasing the TPB density near the electrolyte and anode interface increases the number of sites available for the charge transfer by the AFL, leading to an enhancement in the cell performance.

Magnetron sputtered AFLs can be used to improve the efficiency of various types of cells, such as electrolyte-supported, anode-supported, and micro-SOFC. The only exceptions are metal-supported SOFC, because as-deposited AFLs require annealing in air after deposition.

Acknowledgements

This work was supported by the Russian Science Foundation (grant No. 17-79-30071).

REFERENCES

1. Mahato N., Banerjee A., Gupta A., Omar S., Balani K. Progress in material selection for solid oxide fuel cell technology: A review. *Prog. Mater. Sci.* 2015, vol. 72, pp. 141–337.
2. Kennouche D., Hong J., Noh H.S., Son J.W., Barnett S.A. Three-dimensional microstructure of high-performance pulsed-laser deposited Ni-YSZ SOFC anodes. *Phys. Chem. Chem. Phys.* 2014, vol. 16, no. 29, pp. 15249–15255.
3. Noh H.S., Yoon K.J., Kim B.K., Je H.J., Lee H.W., Lee J.H., Son J.W. The potential and challenges of thin-film electrolyte and nanostructured electrode for yttria-stabilized zirconia-base anode-supported solid oxide fuel cells. *J. Power Sources.* 2014, vol. 247, pp. 105–111.

4. Park J.H., Han S.M., Yoon K.J., Kim H., Hong J., Kim B.K., Lee J.H., Son J.W. Impact of nanostructured anode on low-temperature performance of thin-film-based anode-supported solid oxide fuel cells. *J. Power Sources*. 2016, vol. 315, pp. 324–330.
5. Coddet P., Liao H., Coddet C. A review on high power SOFC electrolyte layer manufacturing using thermal spray and physical vapour deposition technologies. *Adv. Manuf.* 2014, vol. 2, pp. 212–221.
6. Tanhaei M., Mozammel M. Yttria-stabilized zirconia thin film electrolyte deposited by EB-PVD on porous anode support for SOFC applications. *Ceram. Int.* 2017, vol. 43, no. 3, pp. 3035–3042.
7. Hong Y.S., Kim S.H., Kim W.J., Yoon H.H. Fabrication and characterization GDC electrolyte thin films by e-beam technique for IT-SOFC. *Curr. Appl. Phys.* 2011, vol. 11, no. 5, pp. 163–168.
8. Hidalgo H., Reguzina E., Millon E., Thomann A.L., Mathias J., Boulmer-Leborgne C., Sauvage T., Brault P. Yttria-stabilized zirconia thin films deposited by pulsed-laser deposition and magnetron sputtering. *Surf. Coat. Technol.* 2011, vol. 205, no. 19, pp. 4495–4499.
9. De Vero J.C., Develos-Bagarinao K., Matsuda H., Kishimoto H., Ishiyama T., Yamaji K., Horita T., Yokokawa H. Sr and Zr transport in PLD-grown Gd-doped ceria interlayers. *Solid State Ion.* 2018, vol. 314, pp. 165–171.
10. Noh H.S., Son J.W., Lee H., Ji H.I., Lee J.H., Lee H.W. Suppression of Ni agglomeration in PLD fabricated Ni-YSZ composite for surface modification of SOFC anode. *J. Eur. Ceram. Soc.* 2010, vol. 30, pp. 3415–3423.
11. Solovyev A.A., Shipilova A.V., Rabotkin S.V., Ionov I.V., Smolyanskiy E.A. Magnetron deposition of yttria-stabilized zirconia electrolyte for solid oxide fuel cells. *Eurasian Journal of Physics and Functional Materials*. 2018, vol. 2, no. 3, pp. 206–218.
12. Barranco A., Borrás A., Gonzalez-Eliphe A.R., Palmero A. Perspectives on oblique angle deposition of thin films: From fundamentals to devices. *Prog. Mater. Sci.* 2016, vol. 76, pp. 59–153.
13. Rezugina E., Thomann A.L., Hidalgo H., Brault P., Dolique V., Tessier Y. Ni-YSZ films deposited by reactive magnetron sputtering for SOFC applications. *Surf. Coat. Technol.* 2010, vol. 204, pp. 2376–2380.
14. Chawla V., Jayaganthan R., Chandra R. Structural characterizations of magnetron sputtered nanocrystalline TiN thin films. *Mater. Charact.* 2008, vol. 59, pp. 1015–1020.
15. Garcia-Garcia F.J., Yubero F., González-Eliphe A.R., Balomenou S.P., Tsiplakides D., Petrakopoulou I., Lambert R.M. Porous, robust highly conducting Ni-YSZ thin film anodes prepared by magnetron sputtering at oblique angles for application as anodes and buffer layers in solid oxide fuel cells. *Int. J. Hydrog. Energy*. 2015, vol. 40, no. 23, pp. 7382–7387.
16. Muecke U.P., Akiba K., Infortuna A., Salkus T., Stus N.V., Gauckler L.J. Electrochemical performance of nanocrystalline nickel/gadolinia-doped ceria thin film anodes for solid oxide fuel cells. *Solid State Ion.* 2008, vol. 178, pp. 1762–1768.
17. Holzer L., Iwanschitz B., Hocker T., Munch B., Prestat M., Wiedenmann D., Vogt U., Holtappels P., Sfeir J., Mai A., Graule T. Microstructure degradation of cermet anodes for solid oxide fuel cells: quantification of nickel grain growth in dry and in humid atmospheres. *J. Power Sources*. 2011, vol. 196, pp. 1279–1294.
18. Gubner A., Landes H., Metzger J., Seeg H., Stübner, R. Proceedings of the Fifth International Symposium on Solid Oxide Fuel Cells (SOFC-V), Stimming U., Singhal S.C., Tagawa H., Lehnert W., Editors, PV 97-40, pp. 884–850, The Electrochemical Society Proceedings Series, Pennington, NJ 1997.
19. Garcia-Garcia F.J., Yubero F., Espinós J.P., González-Eliphe A.R., Lambert R.M. Synthesis, characterization and performance of robust poison-resistant ultrathin film yttria stabilized zirconia – nickel anodes for application in solid

- electrolyte fuel cells. *J. Power Sources*. 2016, vol. 324, pp. 679–686.
20. Garcia-Garcia F.J., Beltrán A.M., Yubero F., González-Elipé A.R., Lambert R.M. High performance novel gadolinium doped ceria/yttria stabilized zirconia/nickel layered and hybrid thin film anodes for application in solid oxide fuel cells. *J. Power Sources*. 2017, vol. 363, pp. 251–259.
21. Garcia-Garcia F.J., Yubero F., González-Elipé A.R., Lambert R.M. Microstructural engineering and use of efficient poison resistant Au-doped Ni-GDC ultrathin anodes in methane-fed solid oxide fuel cells. *Int. J. Hydrog. Energy*. 2018, vol. 43, pp. 885–893.
22. Tanveer W.H., Ji S., Yu W., Cho G.Y., Lee Y.H., Park T., Lee Y., Kim Y., Cha S.W. Effect of 20% O₂ reactive gas on RF-sputtered Ni-SDC cermet anodes for intermediate temperature solid oxide fuel cells. *Curr. Appl. Phys.* 2016, vol. 16, no. 12, pp. 1680–1686.
23. Jou S., Wu T.H. Thin porous Ni-YSZ films as anodes for solid oxide fuel cell. *J. Phys. Chem. Solids* 2008, vol. 69, pp. 2804–2812.
24. Takagi Y., Adam S., Ramanathan S. Nanostructured ruthenium–gadolinia-doped ceria composite anodes for thin film solid oxide fuel cells. *J. Power Sources*. 2012, vol. 217, pp. 543–553.
25. Ionov I.V., Solovyev A.A., Shipilova A.V., Lebedynskiy A.M., Smolyanskiy E.A., Lauk A.L., Semenov V.A. Reactive co-sputter deposition of nanostructured cermet anodes for solid oxide fuel cells. *Jpn. J. Appl. Phys.* 2018, vol. 57, article number 01AF07.
26. Solovyev A.A., Shipilova A.V., Ionov I.V., Kovalchuk A.N., Rabotkin S.V., Oskirko V.O. Magnetron-sputtered YSZ and CGO electrolytes for SOFC. *J. Electron. Mater.* 2016, vol. 45, pp. 3921–3928.
27. Fukunaga H., Ishino M., Yamada K. Effective thickness of Ni–Sm-doped ceria cermet anode for solid oxide fuel cell. *Electrochem. Solid-State Lett.* 2007, vol. 10, pp. B16–B18.
28. Flytzani-Stephanopoulos M., Sakbodin M., Wang Z. Regenerative adsorption and removal of H₂S from hot fuel gas streams by rare earth oxides. *Science*. 2006, vol. 312, pp. 1508–1510.
29. Papurello D., Lanzini A., Fiorill S., Smeacetto F., Singh R., Santarelli M. Sulfur poisoning in Ni-anode solid oxide fuel cells (SOFCs): deactivation in single cells and a stack. *Chem. Eng. J.* 2016, vol. 283, pp. 1224–1233.
30. Gross M.D., Vohs J.M., Gorte R.J. Recent progress in SOFC anodes for direct utilization of hydrocarbons. *J. Mater. Chem.* 2007, vol. 17, pp. 3071–3077.
31. Lu C., Worrell W.L., Gorte R.J., Vohs J.M. SOFCs for direct oxidation of hydrocarbon fuels with samaria-doped ceria electrolyte. *J. Electrochem. Soc.* 2003, vol. 150, pp. A354–A358.
32. Lee S., Hong H.S., Lee M.J., Woo S.K. Characterization of CuO/YSZ high temperature electrolysis cathode material fabricated by high energy ball-milling: 900 °C reduced by hydrogen exposure. *Mater. Test.* 2014, vol. 56, pp. 40–46.
33. Park S., Gorte R.J., Vohs J.M. Tape cast solid oxide fuel cells for the direct oxidation of hydrocarbons. *J. Electrochem. Soc.* 2001, vol. 148, pp. A443–A447.
34. Benoved N., Kesler O. Air plasma spray processing and electrochemical characterization of Cu–SDC coatings for use in solid oxide fuel cell anodes. *J. Power Sources*. 2009, vol. 193, pp. 454–641.
35. De Marco V., Grazioli A., Sglavo V.M. Production of planar copper-based anode supported intermediate temperature solid oxide fuel cells cosintered at 950 °C. *J. Power Sources*. 2016, vol. 328, pp. 235–240.
36. Azzolini A., Sglavo V.M., Downs J.A. Production and performance of copper-based anode-supported SOFCs. *ECSTrans.* 2015, vol. 68, pp. 2583–2596.

МАГНЕТРОННОЕ ОСАЖДЕНИЕ АНОДНЫХ ФУНКЦИОНАЛЬНЫХ СЛОЕВ ДЛЯ ТВЕРДОКСИДНЫХ ТОПЛИВНЫХ ЭЛЕМЕНТОВ

А.А. Соловьев¹, И.В. Ионов¹, А.В. Шипилова¹, В.А. Семенов¹, Е.А. Смолянский²

¹Институт сильноточной электроники СО РАН,
634055, г. Томск, пр. Академический, 2/3, e-mail: andrewsol@mail.ru

²Томский политехнический университет,
634050, г. Томск, пр. Ленина, 30

Предлагаемый обзор посвящен последним достижениям в области магнетронного осаждения тонкопленочных анодных функциональных слоев (АФС) для твердооксидных топливных элементов (ТОТЭ) различных конструкций (на несущем электролите, на несущем аноде и микро-ТОТЭ). Производство компонентов ТОТЭ остается в настоящее время важным фактором для промышленного развития этого электрохимического устройства. Формирование тонких наноструктурированных анодных слоев методами физического газофазного осаждения позволяет повысить эффективность ТОТЭ за счет уменьшения поляризационных потерь на аноде. В обзоре обсуждается использование тонкопленочных анодов для различных конструкций ТОТЭ, работающих в диапазонах низких, средних и высоких температур. Проанализировано влияние параметров осаждения, микроструктуры и химического состава АФС на характеристики ТОТЭ.

Ключевые слова: *ТОТЭ, анодный функциональный слой, тонкая пленка, магнетронное распыление, поляризационные потери.*

BƏRK OKSİD YANACAQ ELEMENTLƏRİ ÜÇÜN ANOD FUNKSIONAL ÖRTÜKLƏRİN MAQNETRON ÇÖKDÜRÜLMƏSİ

A.A. Solovyov¹, I.V. Ionov¹, A.V. Shipilova¹, V.A. Semenov¹, E.A. Smolyanskiy²

¹Rusiya EA Sibir Bölməsinin Dəqiq elektronika institutu
634055, Rusiya, Tomsk şəh., pr. Akademıçeskiy pr., 2/3, e-mail: andrewsol@mail.ru

²Tomsk politexnik universiteti
634050, Rusiya, Tomsk şəh., Lenin pr., 30

Təqdim olunan icmal müxtəlif konstruksiyalı bərk oksid yanacaq elementləri üçün anod funksional təbəqələrinin maqnetron çökdürmə yolu ilə alınmasına həsr olunub. Nazik nanostrukturlu anod təbəqələrinin qaz fazadan çökdürmə usulu ilə formalaşması bərk oksid yanacaq elementlərinin effektivliyini anodda polyarizasiya itkisinin azalması hesabına artırır.

İcmalda aşağı, orta və yüksək temperatur intervalında işləyən müxtəlif konstruksiyalı bərk oksid yanacaq elementləri üçün nazik təbəqəli anodların istifadəsi müzakirə olunur. Anod funksional təbəqələrinin mikrostrukturunu və kimyəvi təkkibinin, eləcə də çökdürmə parametrlərinin bərk oksid yanacaq elementlərinin xarakteristikalarına təsiri analiz edilib.

Açar sözlər: *anod funksional örtükləri, bərk oksid yanacaq elementləri, maqnetron səpilmə metodu*